Progress In Electromagnetics Research Letters, Vol. 99, 159–167, 2021

A CPW Fed Clown-Shaped Super Wideband Antenna

Rahul K. Garg[1, *], Sarthak Singhal[2], and Raghuvir Tomar[1]

Abstract—A Clown-shaped patch antenna for super wideband applications is presented. The radiator is placed on a 1.6 mm thick RT/Duroid 5880 substrate and is fed using a 50 Ω symmetric coplanar waveguide. The size of the proposed antenna is $26 \times 27\,\text{mm}^2$ ($0.256\lambda_L \times 0.266\lambda_L$, where λ_L is the wavelength at the lower band edge frequency, i.e., 2.96 GHz). The radiator is a combination of an ellipse, a rectangle, and a triangle. An impedance bandwidth of 2.96 GHz to more than 100 GHz (i.e., more than 33.78 : 1 ratio bandwidth) is achieved. Nearly-omnidirectional radiation patterns with an average gain of 6 dBi are achieved. A fractional bandwidth greater than 188.5%, a size reduction of $\sim 97\%$, and a comparable bandwidth dimension ratio of 2768 are achieved. The antenna has additional advantages like compactness, planar geometry, and super-wide bandwidth.

1. INTRODUCTION

In modern wireless communication systems, the increased demands for higher data rates, higher capacity, better security, and higher reliability require wideband antennas with improved radiation characteristics [1–4]. In 2002, the Federal Communication Commission allocated an unlicensed frequency spectrum from 3.1 GHz to 10.6 GHz for ultra-wideband (UWB) communication [5]. This UWB covers short-range communication applications like remote sensing, radar imaging, and wireless personal area networks. Nowadays, the demands for high-resolution public surveillance systems, with better resolution and imaging, are being met using super wideband (SWB) communication. An SWB antenna fulfils the demands of extremely high data rate, high capacity, and high-resolution video transmission. It can be used for both short-range and long-range communications. There is no well-defined range of SWB frequency spectrum yet. Typically, a bandwidth ratio greater than 10:1 is considered to be SWB [6–8]. The patch antenna is a very popular type of microstrip antenna. In the available literature, several patch antenna designs having enhanced bandwidth have already been investigated and reported for super wideband applications [9–26]. These structures have either large dimensions concerning that of compact wireless communication systems, or their operating bandwidth is unable to cover the frequency spectrum beyond 80 GHz.

In the present work, a Clown-shaped antenna having compact dimensions and operating beyond 100 GHz is proposed. The technique of adding semi-elliptical, rectangular, and triangular radiators is utilized to achieve a lower band edge frequency of 2.96 GHz. The combination of coplanar waveguide (CPW) feeding and modified radiator results in SWB characteristics. The antenna is designed using the commercial CST-Microwave studio software. The design has been fabricated and tested. Experimental data are in good agreement with the simulated ones. A detailed performance comparison with other similar published designs is also made.

Received 5 July 2021, Accepted 9 August 2021, Scheduled 21 August 2021

* Corresponding author: Rahul Kumar Garg (rahulkumargarg08@gmail.com).

[1] Department of Electronics and Communication Engineering, The LNM Institute of Information Technology, Jaipur, India.

[2] Department of Electronics and Communication Engineering, Malaviya National Institute of Technology, Jaipur, India.

2. DESIGN AND CONFIGURATION

The proposed Clown-shaped antenna design is shown in Fig. 1(a). The antenna is designed on a 1.6 mm thick RT/Duroid 5880 substrate (dielectric constant of 2.2 and loss tangent of 0.009). This substrate exhibits uniform electrical properties over the frequency band of interest, low moisture absorption, and excellent chemical resistance. Such properties are highly desired in the substrate selection for an SWB antenna.

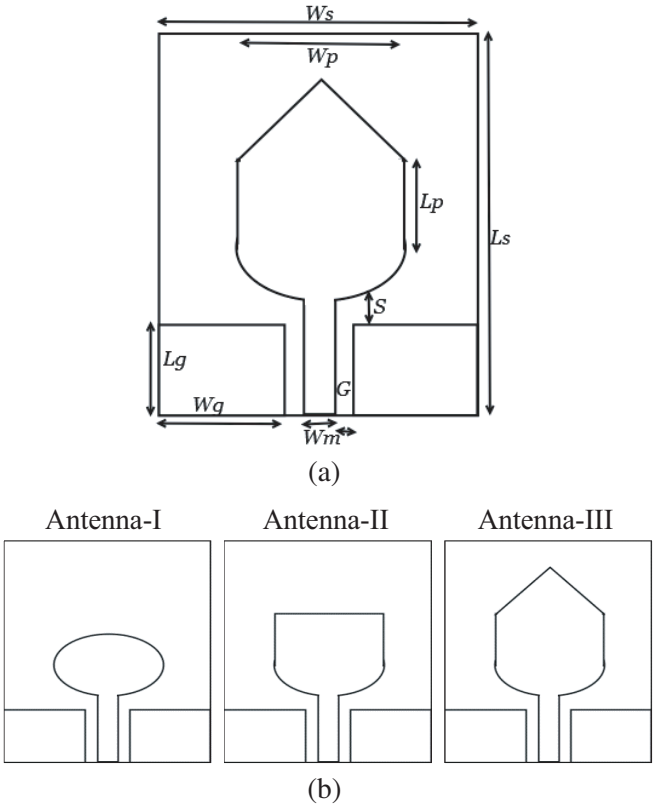

Figure 1. (a) Proposed Clown-shaped super wideband antenna design. (b) Derivation stages of the proposed antenna design.

The proposed design is derived from a semi-elliptical monopole antenna as shown in Fig. 1(b). There are three derivation stages: Antenna-I, Antenna-II, and Antenna-III. In the first stage, i.e., Antenna-I, a CPW fed elliptical monopole antenna was designed. Antenna-II is derived by replacing the upper half of the elliptical radiator with a rectangular radiator. In the last stage, a triangular radiator is mounted on top of the second stage radiator. The elliptical shape near the feed line and ground plane is necessary for good impedance matching over the wide frequency range involved. The additional geometries (rectangular and triangular) introduce additional resonances which help in generating a rational bandwidth greater than 10:1. The optimized design dimensions are $Ls = 27$ mm, $Lm = 6$ mm, $Lg = 5.5$ mm, $Lp = 7$ mm, $G = 0.5$ mm, $Ws = 26$ mm, $Wm = 2$ mm, $Wg = 11.5$ mm, $Wp = 14$ mm, $S = 0.5$ mm.

3. RESULTS AND DISCUSSIONS

The performances of the various derivation stages (Antenna-I, Antenna-II, and Antenna-III) were evaluated for the frequency range of 1 GHz to 40 GHz. The voltage standing wave ratio (VSWR) versus frequency plots for the three derivation stages are compared in Fig. 2(a). It is observed that lower cut-off frequencies are 4.37 GHz, 3.46 GHz, and 2.96 GHz for Antenna-I, Antenna-II, and Antenna-III,

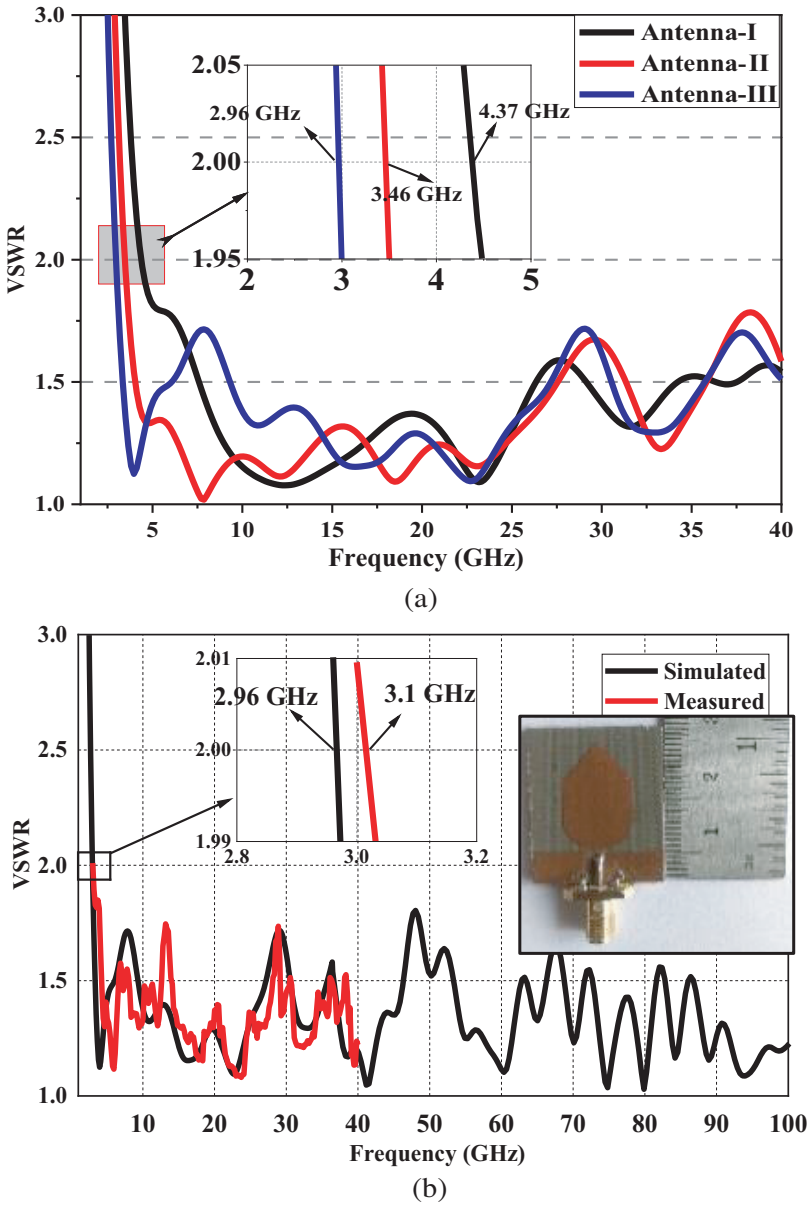

Figure 2. (a) VSWR versus frequency plot for various derivation stages of the proposed antenna, and (b) simulated and measured VSWR versus frequency plot.

respectively. The curvature in the radiating patch near the feed line and ground plane provides the wideband impedance matching (it is observed in the case of Antenna-I). The lower cut-off frequency is directly proportional to the outer dimensions of the radiating patch. In the case of Antenna-II and Antenna-III, with the addition of the rectangular and triangular shapes to the elliptical patch, the resultant outer physical dimension of the proposed patch is increased. The introduction of rectangular and triangular geometries increases the physical dimension and reduces the lower operating frequency of the antenna from 4.37 GHz to 2.96 GHz. It is also observed that the upper cut-off frequencies of all derivation stages are greater than 40 GHz. Simulated results show an extremely large bandwidth of more than 37.04 GHz (2.96 GHz to $>$ 40 GHz). The proposed antenna (Antenna-III) is simulated further to find out the upper cut-off frequency. The simulated results show that the proposed antenna operates well beyond 100 GHz. Due to the limited computational facilities, the proposed antenna was simulated only up to 100 GHz.

To validate the simulated results, the proposed antenna (Antenna-III) was fabricated and tested experimentally by using Performance Network Analyzer (PNA-L) (10 MHz to 43.5 GHz) in an Anechoic Chamber. The measurement was limited to 40 GHz due to the limitation of the measurement setup. A photograph of the fabricated antenna and the measured and simulated VSWR plots are shown in Fig. 2(b). The measured bandwidth is $>$ 36.9 GHz (3.1 GHz to more than 40 GHz). The measured lower cut-off frequency (3.1 GHz) slightly differs from the simulated value, which can be attributed to the uncertainties in the assumed dielectric constant value, fabrication tolerances, etc.

Surface current distributions in the proposed antenna at 3.9 GHz, 10.9 GHz, 16.3 GHz, 22.9 GHz, 32.2 GHz, 41.1 GHz, 60.2 GHz, 70.1 GHz, and 88.7 GHz are shown in Figs. 3(a)–3(i). The frequencies are selected based on the resonance frequencies seen in the VSWR plot. The surface current is distributed all over the patch, feed line, and ground planes. The nature of current distribution depends on the frequency. It is observed that as frequency increases, the higher-order modes are generated which can be visualized in Fig. 3.

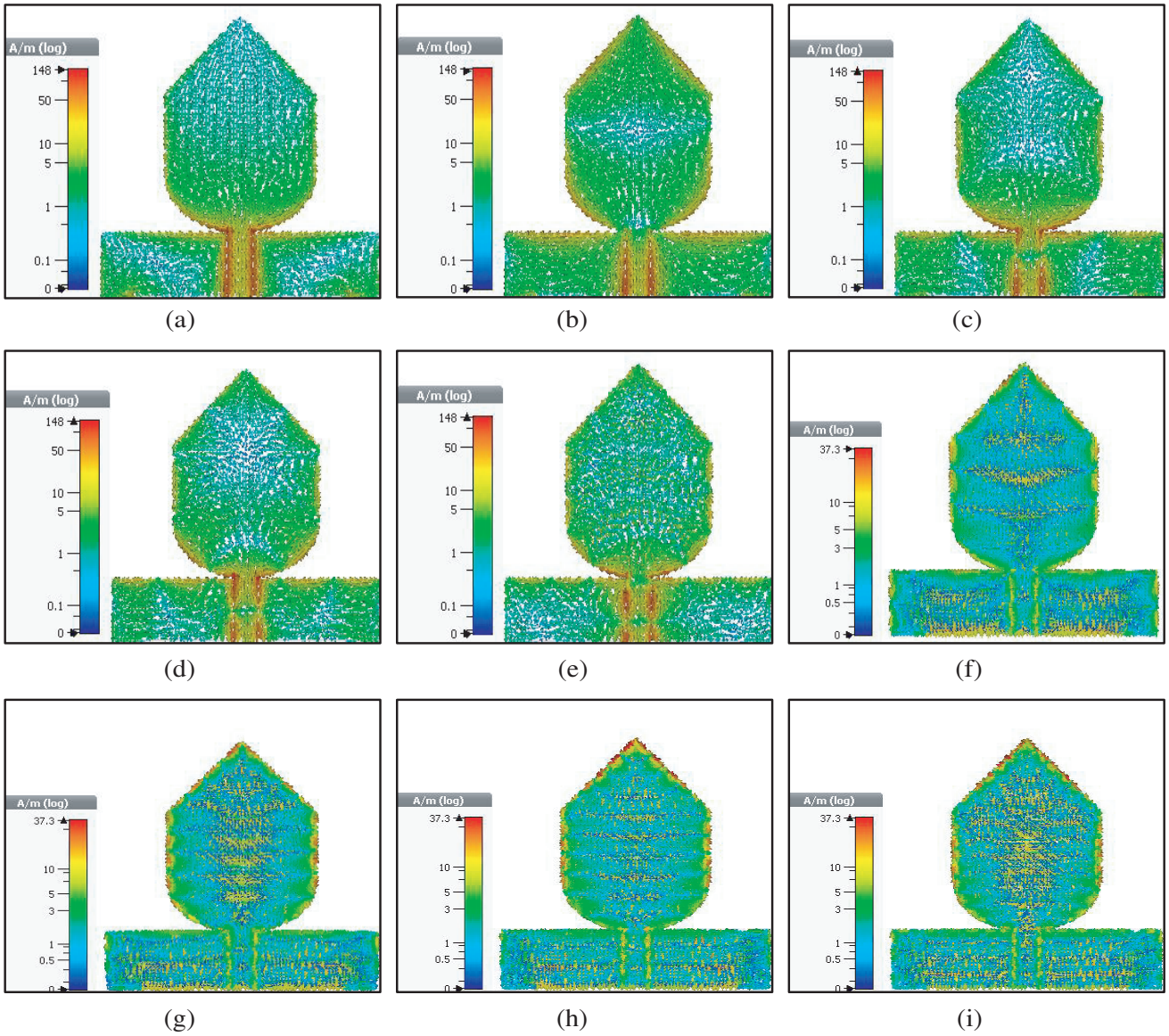

Figure 3. Surface current distributions at few frequencies (a) 3.9 GHz, (b) 10.9 GHz, (c) 16.3 GHz, (d) 22.9 GHz, (e) 32.2 GHz, (f) 41.1 GHz, (g) 60.2 GHz, (h) 70.1 GHz, and (i) 88.7 GHz.

The radiation patterns of the proposed antenna geometry in E-plane (XZ-plane) and H-plane (YZ-plane) were measured only up to 18 GHz due to limitations of experimental facilities. During the radiation pattern measurement in an anechoic chamber, MXG Analog Microwave Signal Generator (frequency range from 100 kHz to 40 GHz) and Waveguide Horn Antenna HF 907 (frequency range from 2 GHz to 18 GHz) were used. The pyramidal horn antenna was used as the transmitting antenna, and the proposed antenna was used as the receiving antenna. A microwave signal generator was connected to the transmitting antenna via an isolator. The receiving antenna was placed in the far-field region and connected to the computerized detection setup. The simulated and measured patterns in E-plane and H-plane at 3.9 GHz, 10.9 GHz, and 16.3 GHz are shown in Figs. 4(a)–4(c). The H-plane radiation patterns are omnidirectional, and the E-plane patterns are bidirectional at lower frequencies. The radiation patterns start distorting as the frequency becomes higher than 15 GHz. This pattern distortion is probably the result of higher-order mode generation and hybrid-mode excitation at those frequencies. The variations of simulated peak gain and efficiency with frequency are plotted in Fig. 4(d). It is observed that the gain increases with an increment in frequency. A 6 dBi peak gain is observed. The total efficiency of the antenna is between 70% and 90%.

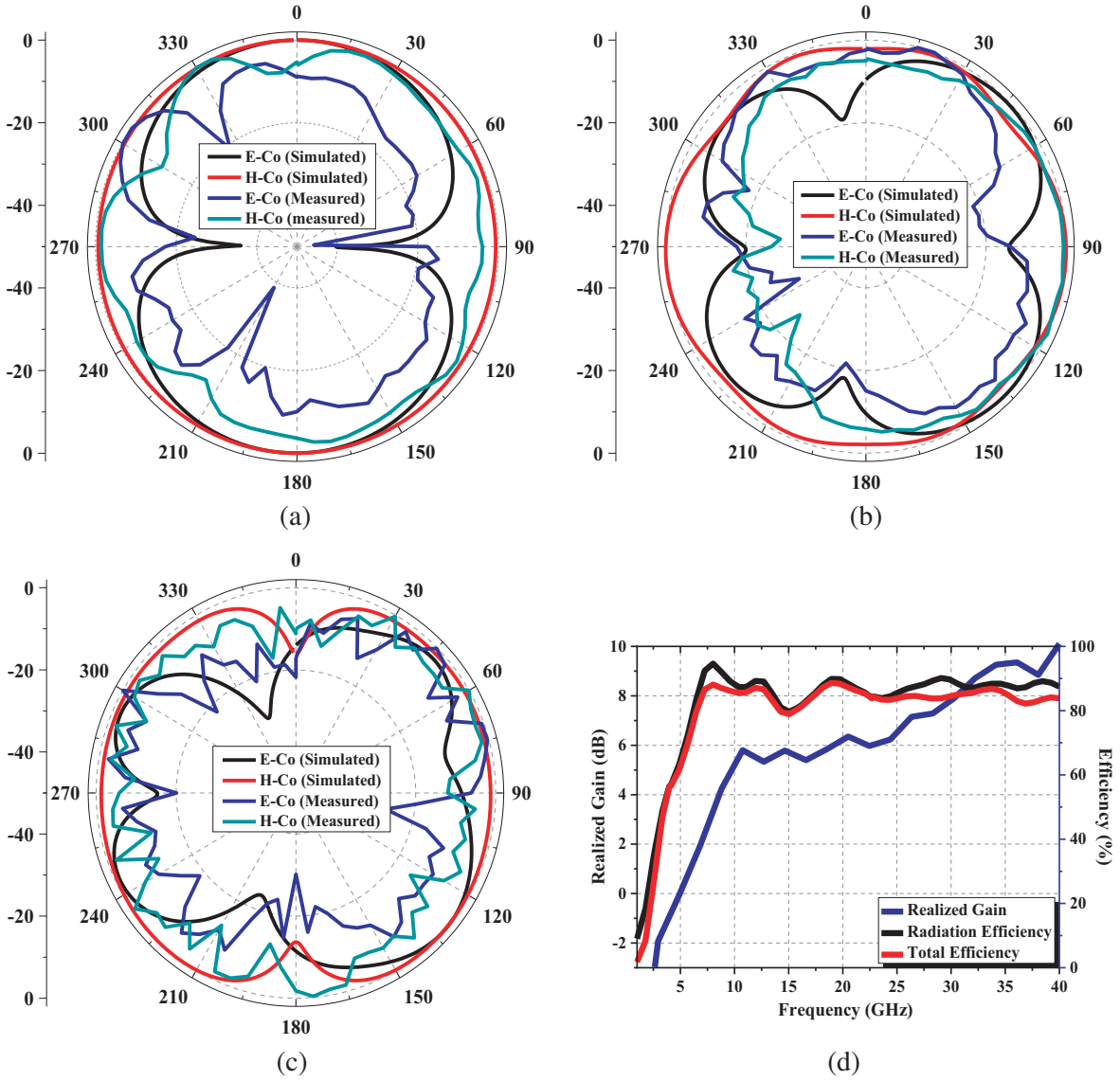

Figure 4. Radiation patterns at (a) 3.97 GHz, (b) 10.88 GHz, and (c) 16.28 GHz, (d) simulated realized gain and efficiency versus frequency graph.

Another performance parameter of the antenna is bandwidth dimension ratio (BDR). BDR is defined as the percentage bandwidth of the antenna per unit area, where the length and width of the antenna are calculated in terms of its highest wavelength (λ_L) corresponding to the lower cut-off frequency. In other words, the formulation for BDR is as follows [10]:

$$BDR = \frac{Percentage\ B.W.}{(\lambda_L \times \lambda_L)} \tag{1}$$

Table 1 presents a comparison between the performance of the proposed and other similar antenna structures. The size of the antenna (in terms of its highest wavelength, λ_L) is calculated at the lower edge frequency of the operating bandwidth. It is observed from this table that the proposed design has a size reduction up to 97% (which is based on the physical dimensions of the reported antenna designs), a comparable percentage bandwidth ($> 188\%$), and a bandwidth ratio of more than $33.78 : 1$. Additionally, BDR for the proposed antenna structure is more than 2768, which is comparable to the BDR reported for other similar designs.

Table 1. Comparison of the proposed antenna with antenna available in the literature.

Antenna	Dimensions		F_L (GHz)	F_H (GHz)	B.W. (GHz)	Fractional B.W. (%)	B.W. Ratio	BDR	% Size Reduction
	mm × mm	($\lambda_L \times \lambda_L$)							
[11]	60 × 40	0.348 × 0.232	1.74	100	98.26	193	57.47	2390	70.7
[12]	43.2 × 38.4	0.18 × 0.16	1.25	40	38.75	187	32	6493	57.6
[13]	34 × 25	0.188 × 0.138	1.66	56.1	54.44	195	33.79	7516	17.41
[14]	29 × 22	0.28 × 0.212	2.9	40	37.1	172	13.79	2897	-
[15]	35 × 35	0.268 × 0.268	2.3	34.8	32.5	175	15.13	2436	42.69
[16]	30 × 30	0.3×0.3	3	20	17	147	6.66	1633	22
[17]	40 × 40	0.345 × 0.345	2.59	31.14	28.55	169	12.02	1306	56.1
[18]	170 × 150	0.368 × 0.325	0.65	35.61	34.96	192	54.78	1605	97.24
Here	**26 × 27**	**0.256 × 0.266**	**2.96**	**> 100**	**> 97.04**	**> 188**	**> 33.78**	**> 2768**	-

4. TIME-DOMAIN ANALYSIS

Besides the frequency domain analysis, time-domain analysis of the SWB antenna is also necessary to evaluate the performance for system applications. SWB system transmits short pulses in place of continuous pulses. For the time-domain analysis, two identical antennas are placed in the same environment in two different configurations named Face-to-Face (F2F) and Side-by-Side (S2S) configurations, respectively. In each configuration, one of the placed antennas works as a transmitting antenna and the other one as a receiving antenna. The distance between the antennas in each configuration was kept fixed at 30 cm which was large enough to ensure that the antennas were in the far-field region of each other. Fidelity factor (F), group delay, isolation ($|S_{21}|$), and phase of the S_{21} are the performance parameters of interest in the time-domain analysis. The correlation between the transmitted and received pulses is represented by the fidelity factor (F). The value of F should be greater than 50% and can be calculated as follows [27].

$$F = \max\left[\frac{\int_{-\infty}^{\infty} S_t(t) S_r(t+\tau) d\tau}{\int_{-\infty}^{\infty} |S_t(t)|^2\, dt \int_{-\infty}^{\infty} |S_r(t)|^2\, dt}\right] \tag{2}$$

The time delay of an impulse signal at the receiver end at different frequencies is measured by group delay. The group delay should be less than 5 ns, ideally speaking [27, 28]. Pulse handling capability is measured by using the transfer function or transmission loss ($|S_{21}|$), and the linear variation in phase of S_{21} indicates an absence of the out-of-phase components in the received signal. Time-domain performance parameter analysis of the proposed antenna is shown in Fig. 5.

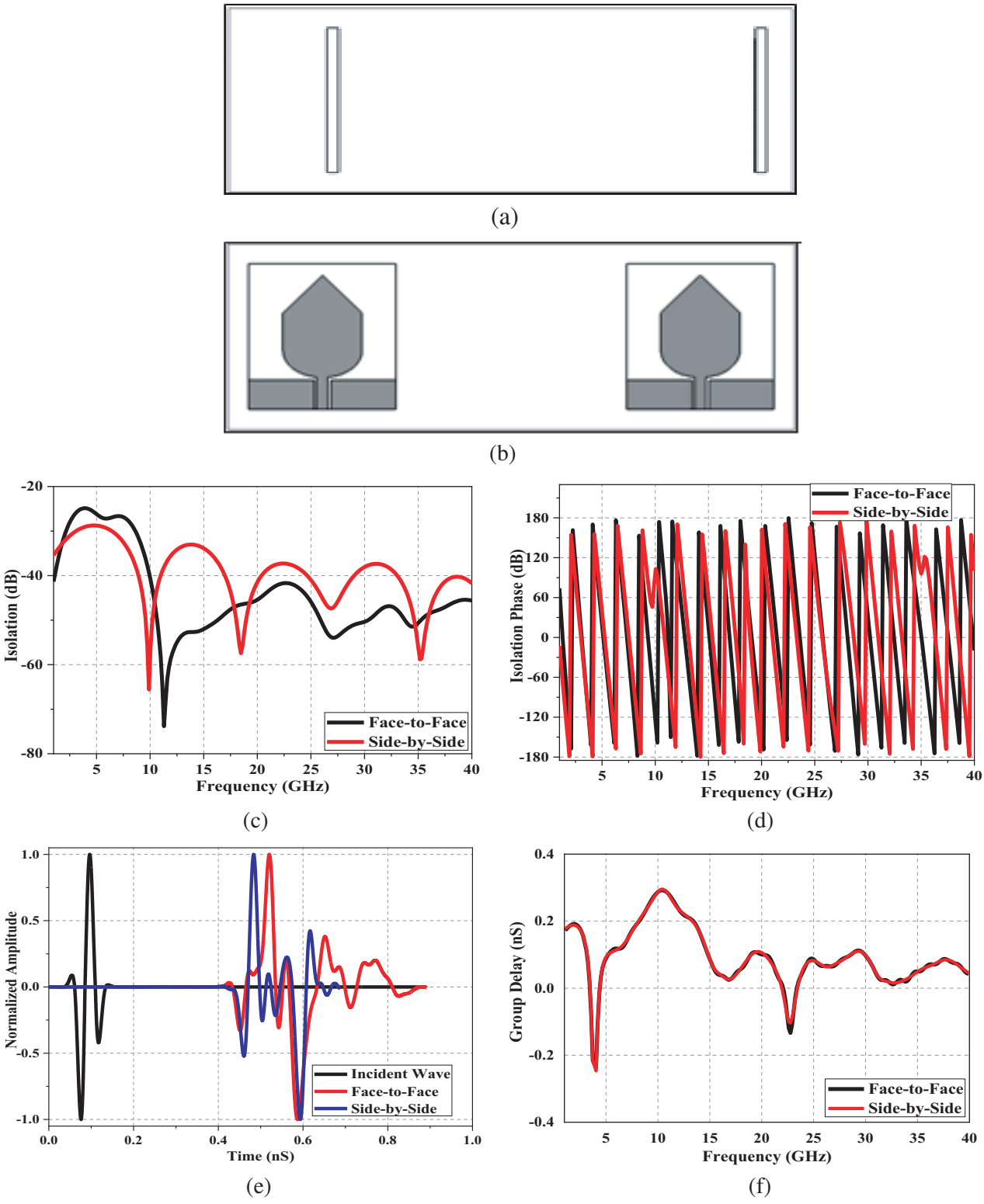

Figure 5. Time-domain analysis. (a) Face-to-Face configuration, (b) Side-by-Side configuration, (c) isolation, (d) isolation phase, (e) transmitted and received pulse normalized amplitudes, and (f) group delay.

The calculated F is 70.9% for the F2F configuration and 78.2% for the S2S configuration. The group delay versus frequency diagrams of both configurations overlap with each other. The value of group delay obtained is 0.3 ns, which is within the allowable limits of 5 ns. The isolation is better than 25 dB in each configuration and goes up to 75 dB, ensuring very good isolation. The phase of the S_{21} varies linearly with the frequency. This signifies the absence of out-of-phase components in received pulses for both configurations.

5. CONCLUSION

A new coplanar waveguide fed Clown-shaped patch antenna for super wideband applications is presented. The introduction of rectangular and triangular geometries reduces the lower operating frequency of the antenna. The proposed antenna shows a super-wide bandwidth of 2.96 GHz to more than 100 GHz in simulation. A fractional bandwidth greater than 188.5%, a size reduction of $\sim 97\%$, and a comparable bandwidth dimension ratio of ~ 2768 are achieved. The antenna is fabricated and tested experimentally. The measured and simulated data are in good agreement. The antenna exhibits advantages like compactness, planar geometry, and super-wide bandwidth. This antenna will find many applications in WLAN, WiMAX, C, S, X, K, and Ku band systems.

ACKNOWLEDGMENT

The authors acknowledge the help and support provided by the Department of Electronics and Communication Engineering, Government Women Engineering College, Ajmer, and convey sincere thanks to the organization.

REFERENCES

1. Schantz, H. G., "A brief history of UWB antennas," *IEEE Aerospace and Electronic Systems Magazine*, Vol. 19, No. 4, 22–26, 2004.
2. Wiesbeck, W., G. Adamiuk, and C. Sturm, "Basic properties and design principles of UWB antennas," *Proceedings of the IEEE*, Vol. 97, No. 2, 372–385, 2009.
3. Electronic Communications Committee, "The European table of frequency allocations and applications in the frequency range 8.4 kHz to 3000 GHz," *European Conf. Postal and Telecommunications Administrations*, 132–133, February 2013.
4. Rao, Q. and W. Geyi, "Compact multi-band antenna for handheld devices," *IEEE Transactions on Antennas and Propagation*, Vol. 57, No. 10, 3337–3339, 2009.
5. Standard, F.C.C., "First-order and report, revision of part 15 of the commission's rules regarding UWB transmission systems," 2002.
6. Balani, W., M. Sarvagya, T. Ali, P. M. M. Manohara, and S. Das, "Design techniques of super wideband antenna-existing and future prospective," *IEEE Access*, Vol. 7, 141241–141257, 2019.
7. Tran, D., P. Aubry, A. Szilagyi, I. E. Lager, O. Yarovyi, and L. P. Ligthart, "On the design of a super wideband antenna," *Ultra Wideband*, 399–427, Intech Open Limited, London, U.K., 2010.
8. Dong, Y., W. Hong, L. Liu, Y. Zhang, and Z. Kuai, "Performance analysis of a printed super-wideband antenna," *Microwave and Optical Technology Letters*, Vol. 51, No. 4, 949–956, 2009.
9. Chaudhary, A. K. and M. Manohar, "design and analysis of a compact wideband monopole patch antenna for future handheld gadgets," *Progress In Electromagnetics Research C*, Vol. 109, 227–241, 2021.
10. Singhal, S., "Feather-shaped super wideband MIMO antenna," *International Journal of Microwave and Wireless Technologies*, 1–9, 2020.
11. Dey, S., Md. S.Arefin, and N. C. Karmakar, "Design and experimental analysis of a novel compact and flexible super wide band antenna for 5G," *IEEE Access*, Vol. 9, 46698–46708, 2021.
12. Balani, W., M. Sarvagya, A. Samasgikar, T. Ali, and P. Kumar, "Design and analysis of super wideband antenna for microwave applications," *Sensors*, Vol. 21, No. 2, 477, 2021.

13. Hasan, Md R., M. A. Riheen, P. Sekhar, and T. Karacolak, "Compact CPW-fed circular patch flexible antenna for super-wideband applications," *IET Microwaves, Antennas & Propagation*, Vol. 14, No. 10, 1069–1073, 2020.
14. Yu, C., S. Yang, Y. Chen, W. Wang, L. Zhang, B. Li, and L. Wang, "A super-wideband and high isolation MIMO antenna system using a windmill-shaped decoupling structure," *IEEE Access*, Vol. 8, 115767–115777, 2020.
15. Alluri, S. and N. Rangaswamy, "Compact high bandwidth dimension ratio steering-shaped super wideband antenna for future wireless communication applications," *Microwave and Optical Technology Letters*, Vol. 62, No. 12, 3985–3991, 2020.
16. Elhabchi, M., M. N. Srifi, and R. Touahni, "A novel modified U-shaped microstrip antenna for Super Wideband (SWB) applications," *Analog Integrated Circuits and Signal Processing*, 1–8, 2020.
17. Okan, T., "A compact octagonal-ring monopole antenna for super wideband applications," *Microwave and Optical Technology Letters*, Vol. 62, No. 3, 1237–1244, 2020.
18. Singhal, S. and A. K. Singh, "Elliptical monopole based super wideband fractal antenna," *Microwave and Optical Technology Letters*, Vol. 62, No. 3, 1324–1328, 2020.
19. Bhattacharya, A., B. Roy, and A. K. Bhattacharjee, "Compact, isolation enhanced, band-notched SWB-MIMO antenna suited for wireless personal communications," *Wireless Personal Communications*, 1–18, 2020.
20. Rahman, S. U., Q. Cao, H. Ullah, and H. Khalil, "Compact design of trapezoid shape monopole antenna for SWB application," *Microwave and Optical Technology Letters*, Vol. 61, No. 8, 1931–1937, 2019.
21. Figueroa-Torres, C. Á., J. L. Medina-Monroy, H. Lobato-Morales, R. A. Chávez-Pérez, and A. Calvillo-Téllez, "A novel fractal antenna based on the Sierpinski structure for super wide-band applications," *Microwave and Optical Technology Letters*, Vol. 59, No. 5, 1148–1153, 2017.
22. Singhal, S. and A. K. Singh, "Asymmetrically CPW-fed circle inscribed hexagonal super wideband fractal antenna," *Microwave and Optical Technology Letters*, Vol. 58, No. 12, 2794–2799, 2016.
23. Manohar, M., R. S. Kshetrimayum, and A. K. Gogoi, "Printed monopole antenna with tapered feed line, feed region, and patch for super wideband applications," *IET Microwaves, Antennas & Propagation*, Vol. 8, No. 1, 39–45, 2014.
24. Okas, P., A. Sharma, and R. K. Gangwar, "Circular base loaded modified rectangular monopole radiator for super wideband application," *Microwave and Optical Technology Letters*, Vol. 59, No. 10, 2421–2428, 2017.
25. Okas, P., A. Sharma, G. Das, and R. K. Gangwar, "Elliptical slot-loaded partially segmented circular monopole antenna for super wideband application," *AEU — International Journal of Electronics and Communications*, Vol. 88, 63–69, 2018.
26. Okas, P., A. Sharma, and R. K. Gangwar, "Super-wideband CPW fed modified square monopole antenna with stabilized radiation characteristics," *Microwave and Optical Technology Letters*, Vol. 60, No. 3, 568–575, 2018.
27. Quintero, G., J. F. Zurcher, and A. K. Skrivervik, "System Fidelity factor: A new method for comparing UWB antennas," *IEEE Transactions on Antennas and Propagation*, Vol. 59, No. 7, 2502–2512, 2011.
28. Kwon, D.-H., "Effect of antenna gain and group delay variations on pulse-preserving capabilities of ultra-wideband antennas," *IEEE Transactions on Antennas and Propagation*, Vol. 54, No. 8, 2208–2215, 2006.